REPORT DOCUMENTATION PAGE

Form Approved
OMB NO. 0704-0188

1. AGENCY USE ONLY (Leave Blank)	2. REPORT DATE 06/06/06	3. REPORT TYPE AND DATES COVERED **Final Project Report,** 14 Apr 03 - 13 Dec 06

4. TITLE AND SUBTITLE
Multifunctional carbon nanotube damping films

5. FUNDING NUMBERS
ARO Proposal Number: 44112-EG
Agreement Number: DAAD19-03-1-0036

6. AUTHOR(S)
Nikhil Koratkar, Prabhat Hajela and Pulickel Ajayan

7. PERFORMING ORGANIZATION NAME(S) AND ADDRESS(ES)
Rensselaer Polytechnic Institute, 110 8th Street Troy, NY, 12180

8. PERFORMING ORGANIZATION REPORT NUMBER

9. SPONSORING / MONITORING AGENCY NAME(S) AND ADDRESS(ES)
U. S. Army Research Office
P.O. Box 12211
Research Triangle Park, NC 27709-2211

10. SPONSORING / MONITORING AGENCY REPORT NUMBER
44112.3-EG

11. SUPPLEMENTARY NOTES
The views, opinions and/or findings contained in this report are those of the author(s) and should not be construed as an official Department of the Army position, policy or decision, unless so designated by other documentation.

12 a. DISTRIBUTION / AVAILABILITY STATEMENT	12 b. DISTRIBUTION CODE
Approved for public release; distribution unlimited.	

13. ABSTRACT (Maximum 200 words)

The objective of this project was to quantify the energy dissipation that occurs when the interfacial slip of nanoscale fillers is activated in a host matrix material. We consider both polymer (such as polycarbonate, PEO, PEG) and epoxy matrices. The nanoscale fillers considered are carbon nanotubes (both singlewalled as well as multi-walled) as well as fullerenes. The nano-composites are fabricated by using a solution mixing technique with tetra-hydro-furan as the solvent. The interfacial friction damping is quantified by performing uniaxial dynamic load tests and measuring the material storage and loss modulus. We study various effects such as impact of nanotube weight fraction, nanotube surface treatment (oxidation, epoxidation etc.), test frequency, strain amplitude, operating temperature as well as effect of pre-strain or biased strain. The effect of geometry (i.e. aspect ratio) is also considered by comparing the damping response of fullerene-composites with that of nanotube-composites.

14. SUBJECT TERMS	15. NUMBER OF PAGES
Carbon Nanotubes, Structural Damping, Vibration Control, Nano-Composites	16. PRICE CODE

17. SECURITY CLASSIFICATION OR REPORT	18. SECURITY CLASSIFICATION ON THIS PAGE	19. SECURITY CLASSIFICATION OF ABSTRACT	20. LIMITATION OF ABSTRACT
UNCLASSIFIED	**UNCLASSIFIED**	**UNCLASSIFIED**	**UL**

NSN 7540-01-280-5500

Standard Form 298 (Rev.2-89)
Prescribed by ANSI Std. 239-18
298-102

Table of Contents

Final Project Report

Statement of Problem

The objective of this project was to quantify the energy dissipation that occurs when the interfacial slip of nanoscale fillers is activated in a host matrix material. We consider both polymer (such as polycarbonate, PEO, PEG) and epoxy matrices. The nanoscale fillers considered are carbon nanotubes (both singlewalled as well as multi-walled) as well as fullerenes. The nano-composites are fabricated by using a solution mixing technique with tetra-hydro-furan as the solvent. The interfacial friction damping is quantified by performing uniaxial dynamic load tests and measuring the material storage and loss modulus. We study various effects such as impact of nanotube weight fraction, nanotube surface treatment (oxidation, epoxidation etc.), test frequency, strain amplitude, operating temperature as well as effect of pre-strain or biased strain. The effect of geometry (i.e. aspect ratio) is also considered by comparing the damping response of fullerene-composites with that of nanotube-composites.

The results of the study indicate that interfacial slip of the nanoscale fillers in the matrix is highly dependent on the applied strain amplitude. At the low strain amplitudes the nanotubes remain bonded with the matrix and a significant increase in stiffness (storage modulus) is observed. As the strain amplitude is increased interfacial sliding of the nanoscale fillers is activated and the damping (or loss modulus) increases while the storage modulus decreases. Both temperature and pre-strain were found to facilitate the activation of interfacial slip at a relatively lower strain level, while covalent bonding at the nanofiller-matrix junctions was found to inhibit the sliding of the fillers. Test fre-

quency did not play a significant role in the 1-10 Hz range. High aspect ratio fillers such as nanotubes gave much larger damping increases in comparison to fullerenes. The dispersion of the nanotubes in the matrix was also shown to be very important in terms of maximizing the damping levels. Surface treatment such as oxidation of the fillers was found to greatly enhance the dispersion quality. For the high aspect ratio oxidized nanotube fillers we demonstrated greater than one order of magnitude (> 1000%) increase in loss modulus over the pure matrix for 2% weight fraction of the filler materials. These results indicate that non-intrusive carbon nanotube fillers could be used to engineer high levels of structural damping in composite structures. High damping levels will reduce vibration and noise, minimize dynamic stresses, provide aeroelastic stability, and improve performance, safety and reliability in a variety of aerospace, mechanical and civil systems.

Additional details regarding the above are provided in the following sections:

Summary of Results

Materials

A schematic diagram for preparation of singlewalled carbon nanotubes (SWNT) and bisphenol-A-polycarbonate (Lexan 121, General Electric) nanocomposites is shown in figure 1. Bisphenol-A-polycarbonate (figure 2) is by far the most utilized and, therefore, intensively studied variety of polycarbonates. High impact strength, good ductility, high glass transition and melting temperatures make it a valuable material for industrial applications. Polycarbonate has a density of 1.2 gram/cm^3 which is similar to that of purified singlewalled carbon nanotubes (~1.3 gram/cm^3). Therefore the weight fractions quoted in all subsequent sections are approximately equal to the volume fraction of the nanotube fillers in the polycarbinate matrix. In this study, purified HiPCO SWNTs were purchased from Carbon Nanotechnologies Inc., with an average length of 1 μm and average diameter of 1.4 nm. A solution mixing process with Tetrahydrofuran (THF) as the solvent was used to disperse the SWNT in the polymer matrix. Note that because THF is a moderate solvent for polycarbonate (PC), it limits the interaction energy between the polymer and the solvent and encourages the physical adsorption of the polymer onto the nanotube surface. The absorbed polymer serves as a surfactant for dispersing the nanotubes in the solution and then in the polycarbonate matrix, and also as a load transfer agent from the bulk polymer to the nanotubes.

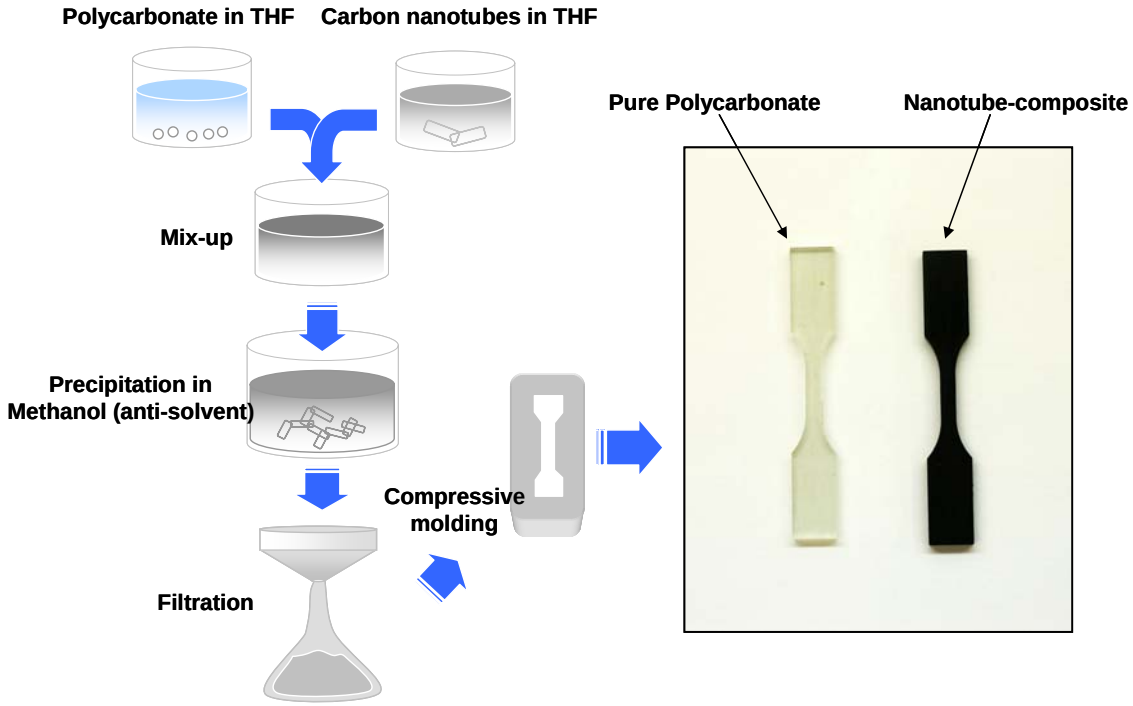

Figure 1: Schematic of the protocol used for SWNT-PC composite sample preparation.

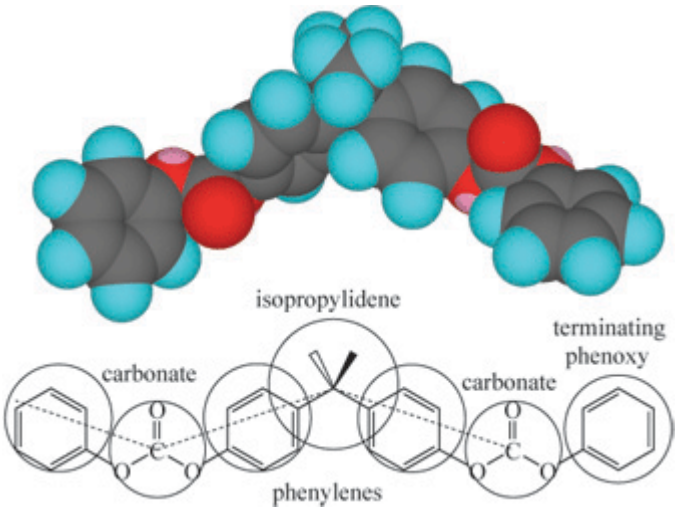

Figure 2: Schematic of the chemical structure of Bisphenol A polycarbonate.

Composite preparation

The SWNTs were first sonicated in THF and polycarbonate was dissolved separately in THF. The SWNT dispersion and PC solution were then mixed in a ratio that resulted in the required SWNT concentration in the polymer, and the mixture was sonicated (750W, 20 KHz) for 15 minutes. To obtain the SWNT-PC nanocomposite, the mixture was poured very slowly into methanol (methyl alcohol, anhydrous). The volume ratio between THF and methanol was 1:5. The composite material precipitated immediately (since methanol is an anti-solvent for polycarbonate) and was filtered and dried out under vacuum for 14 hours. A compressive mold (pre-heated to 205º C) was used to prepare the standard tensile (dog-bone shaped) specimens. The samples (figure 1) have dimensions of ~ 3.2 mm (width), 3.2 mm (thickness) and 63.25 mm in length. The weight fraction of SWNT in the nano-composite was varied between 0.5 and 2%. Pure polycarbonate samples (without nanotube fillers) of the same dimensions were also prepared (following protocol of figure 1) to compare the response of the two materials. Figure 3 shows typical Scanning Electron Microscopy (SEM) images of the fracture surface for SWNT-PC composite with 1.5% weight fraction of as-received SWNT. As seen in the SEM images, SWNT fibers are dispersed in the polymer matrix and are pulling out of the fracture surface. Each nanotube fiber is comprised of a bundle of SWNTs (~ 35 nm in diameter) and appears to be coated with a polymer layer.

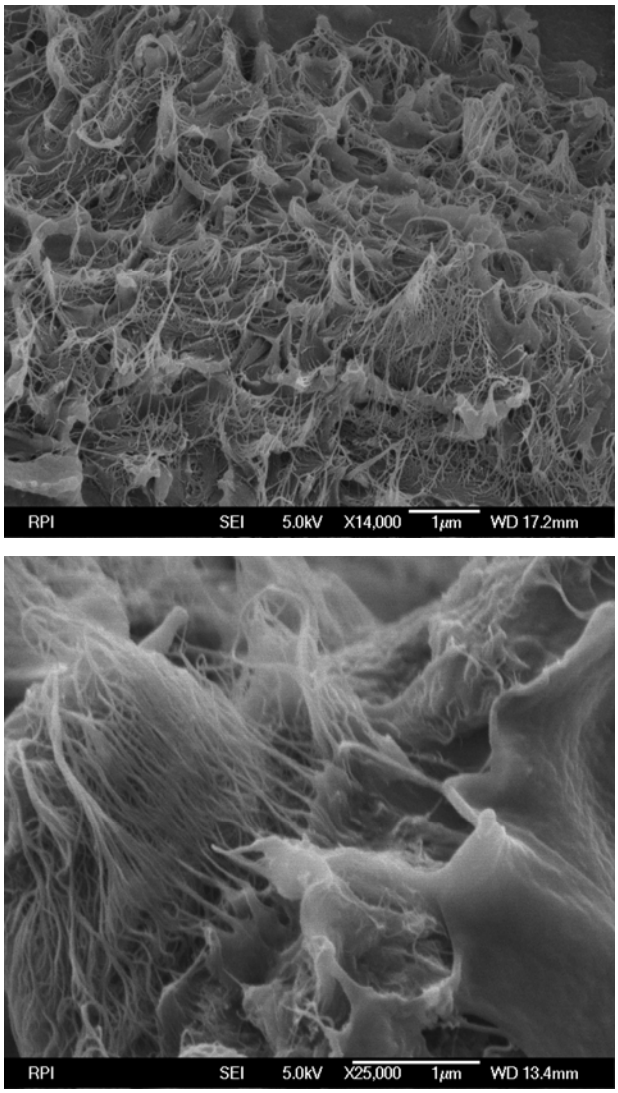

Figure 3: SEM Micrograph of the fracture surface on the composite, showing SWNT fibers dispersed in the polycarbonate matrix. Weight fraction of the nanotubes in the composite is 1.5%.

Dynamic Cyclic Tests

Figure 4 shows a schematic for the viscoelastic characterization of SWNT-PC nanocomposites. The samples are tested under uniaxial cyclic loading using an MTS-858 servo-hydraulic test system (figure 5). All tests in this study are performed at room temperature. Dynamic strain and stress data are measured using an MTS 632.26E-20 extensometer and the load cell of MTS-858 system. In order to characterize and quantify the damping behavior, the linearized material complex modulus was calculated using the measured uniaxial stress (σ) and corresponding strain (ε) response. The linearized stress-strain relation can be expressed as $\sigma = (E' + jE'')\varepsilon$, where the in-phase component (E') determines the storage or elastic modulus (i.e. real part of complex modulus) and the quadrature component (E'') determines the loss modulus (i.e. imaginary part of complex modulus). To obtain the storage and loss moduli, sinusoidal (or oscillatory) strains (figure 4) are applied to the composite sample: $\varepsilon = \varepsilon_0 \sin(\omega t)$, and we measured the resulting stress response, $\sigma = (\sigma_0 \cos\delta) \sin(\omega t) + (\sigma_0 \sin\delta) \cos(\omega t)$, where $\sigma_s = \sigma_0 \cos\delta$ represents the component of the stress that is in phase with the strain and $\sigma_c = \sigma_0 \sin\delta$ represents the component of the stress that is out of phase with respect to the strain. Note that σ_0 is the amplitude of the stress, ω is the angular frequency of the applied strain and δ is a phase angle related to material viscoelasticity. The Fourier transform method was used to obtain the in-phase (σ_s) and out-of-phase (σ_c) components of the measured uniaxial stress response in the frequency domain. The elastic and loss moduli were then calculated as follows: $E' = \sigma_s / \varepsilon_0$ and $E'' = \sigma_c / \varepsilon_0$.

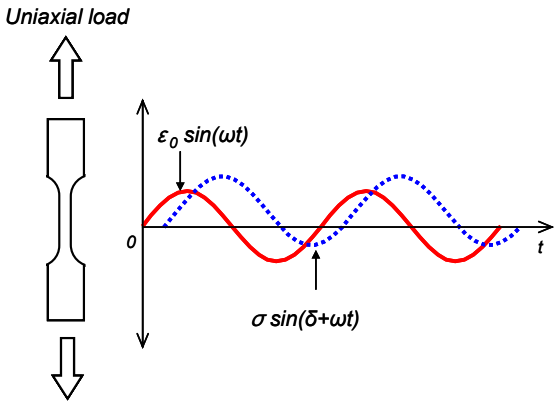

Figure 4: Schematic of the viscoelastic uniaxial mode testing of the SWNT-PC nanocomposite sample. Tests are conducted over a range of strain amplitudes (up to 1.3%) and frequencies (1-10 Hz). All tests are performed at room temperature.

Figure 5: Photograph of MTS 858 Hydraulic-Servo Test System.

Complex Modulus Results

Figures 6a and 6b compare the data for storage and loss moduli of SWNT-PC composite and pure polycarbonate as a function of strain amplitude (test frequency is 10 Hz). The weight fraction of SWNT in the composite is 1.5%. The maximum applied strain amplitude in the test is limited to 1.3% to stay within the elastic region of the polycarbonate. Figure 6a indicates that the elastic modulus of the nanocomposite shows a marked decrease with increasing strain amplitude, indicating that the fiber-matrix reinforcement effect is degrading at large strain levels. This suggests that as the strain amplitude is increased the critical interfacial shear stress for nanotube-polymer interfacial slip is reached and filler-matrix sliding is activated resulting in a decrease in stiffness. This loss in reinforcement with increasing strain amplitude is a gradual process (figure 6a) because not all the nanotube-polymer interfaces will fail simultaneously. Since the nanotube distribution in the polymer is random (no preferred orientation) those tubes that are better aligned with the loading direction tend to fail first. As the strain level is increased more and more of the interfaces begin to fail resulting in a progressive reduction in the reinforcement effect. As frictional sliding at the tube-polymer interfaces is activated, an increase in the loss modulus of the nanocomposite sample is expected. This is clearly seen in figure 6b, which shows that the decrease in elastic modulus with increasing strain is mirrored by a corresponding increase in the loss modulus. A loss modulus of ~ 45 MPa (corresponds to 250% increase compared to the baseline PC) is achieved at about 1.2% strain. In contrast, the pure polycarbonate sample shows strain-

independent loss moduli (~12 MPa) over the entire strain range. The chains of the polycarbonate are highly entangled, so expectedly there is no noticeable interfacial slip between the chains at room temperature. Note that below about 0.2% strain amplitude, the loss modulus of the nanocomposite sample was similar to the baseline PC, which confirms that fiber-matrix sliding is not fully activated at low strain amplitudes. Above about 1% strain level, the loss modulus response plateaus (levels off) indicating that fiber-matrix slip has been activated for a majority of nanotubes in the composite. Also, we investigated the effect of test frequency on tube-polymer frictional sliding mechanism. The test frequency was varied in the 0.01-10 Hz frequency range (figure 7a and 7b); at lower test frequencies enhanced damping behavior for both pure polycarbonate and nanocomposite samples was observed (figure 7a). The reason for this is that at very low test frequencies the system has more time to dissipate the frictional energy resulting from interfacial sliding. However, no strong frequency-dependent behavior is observed for both samples in the 1-10 Hz range.

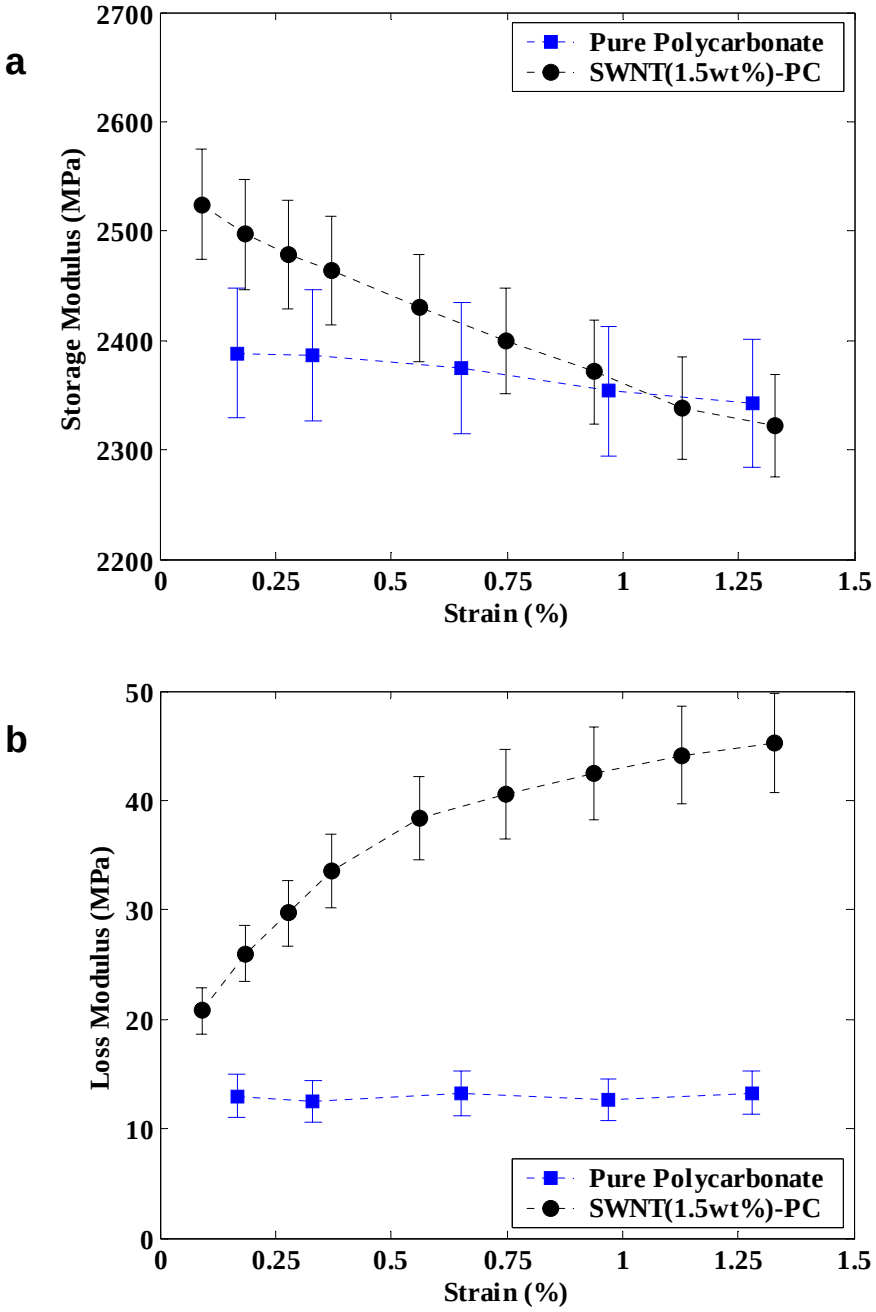

Figure 6: Storage (a) and loss moduli (b) as a function of strain amplitude for 1.5wt% as-received SWNT-PC nanocomposite and pure polycarbonate. (Test frequency: 10 Hz).

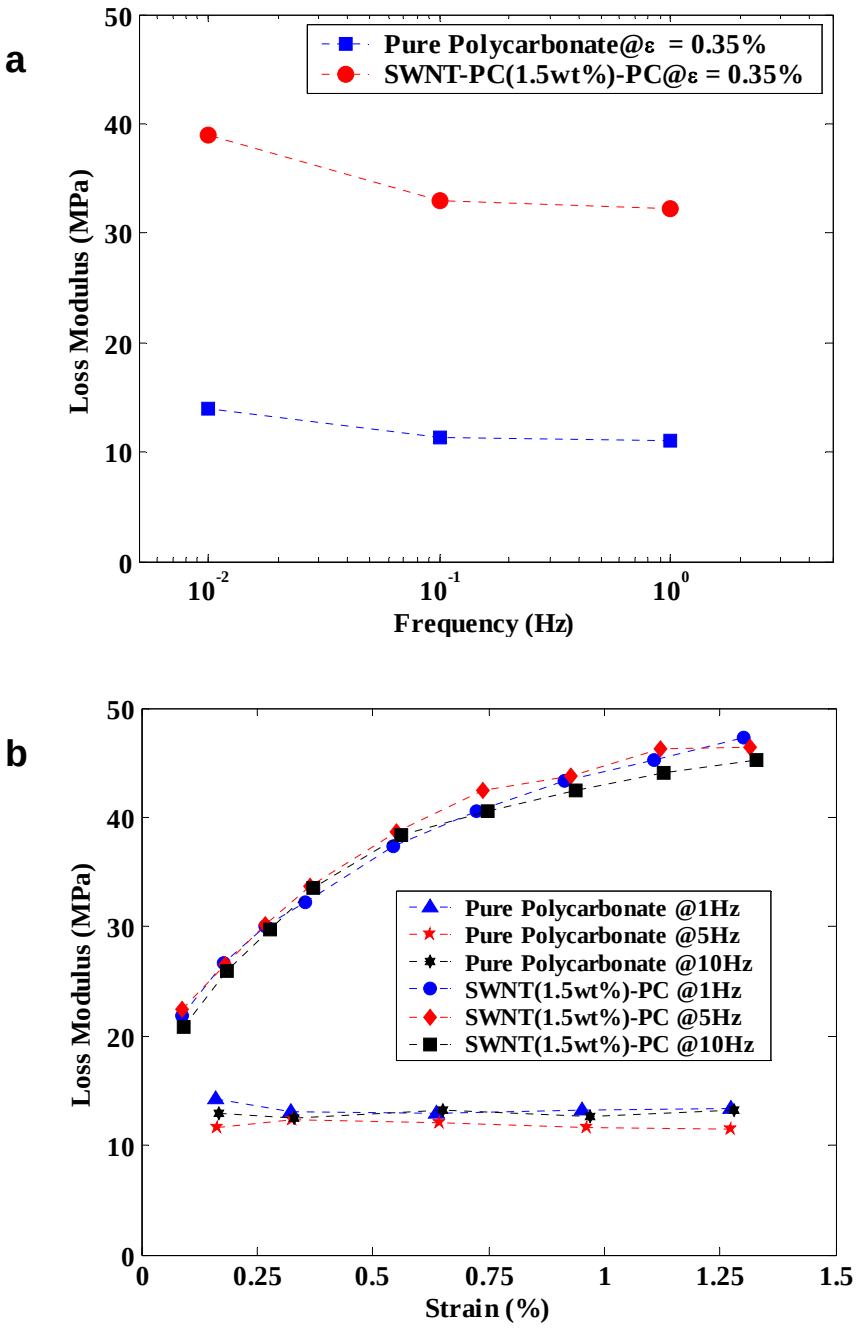

Figure 7: Effect of test frequency on the loss moduli (a) as a function of test frequency (between 0.01 to 1Hz). (b) Response in 1-10 Hz range as a function of strain amplitude for 1.5wt% as-received SWNT-PC nanocomposite and pure polycarbonate.

A shear lag analysis was carried out to estimate the interfacial nanotube-matrix

shear stress needed to activate filler-matrix sliding for the system. The predicted interfacial shear stress is about 20 MPa. This result is similar to recent measurements performed by the Wagner group which indicates that the critical shear stress for interfacial slip at the nanotube-polymer interface (for polyethylenebutene) is in 40-50 MPa range. In contrast to this, slip at the nanotube-nanotube interface is shown to be activated at critical stress levels of only ~ 0.5 MPa. Given that for the composite system, in this study, about 20 MPa stress is required to fully activate the sliding mechanism, it would appear unlikely that tube-tube sliding is playing a significant role. The more plausible scenario is that interfacial sliding at the nanotube-polymer interfaces seems to be the dominant mechanism for the observed increase in energy dissipation.

To confirm that tube-polymer frictional sliding is responsible for the observed increase in damping, a series of control experiments were performed with varying levels of nanotube dispersion. In the first experiment a SWNT-PC composite (with 1.5% weight fraction of nanotubes) is fabricated under reduced sonication time and tested. This composite (with sonication time: 2 minutes) should have larger clusters (bundles) of nanotubes, compared to the control sample (with sonication time: 15 minutes). If tube-tube sliding were the dominant mechanism then the larger nanotube clusters would provide a greater number of tube-tube contacts, thereby enhancing energy dissipation. Expectedly, SEM images (figure 8a) of the fracture surface indicate poor nanotube dispersion and presence of larger clusters of nanotubes in the sample which has less sonication time compared to the control sample (figure 3). Despite having greater tube-tube contacts and more interfaces between individual nanotubes, the loss modulus for the

sample with reduced sonication time is significantly decreased (figure 8b) compared to the control sample. This result indicates that the dominant mechanism for damping in the composite system appears to be frictional sliding at the nanotube-polymer interfaces and not the nanotube-nanotube interfaces.

In a second set of control experiments, multiwalled carbon nanotubes (MWNTs) were dispersed in the polycarbonate matrix. With MWNT the dispersion down to the single tube level (see figure 9a) was achieved using the solution mixing technique outlined in figure 1. Therefore for MWNT-PC composites, all external tube-tube contacts can be virtually eliminated. Even though tube-tube contacts internal to an MWNT still exist, these are not expected to be significant because of weak interaction between concentric cylinders within an MWNT. Figure 9b shows the damping response for the MWNT-PC system with 5% weight fraction of MWNT fillers. For the MWNT-PC composite a higher weight fraction of nanotubes was chosen, compared to the previous SWNT testing because only the outer shells of each individual MWNT are in contact with the matrix. In spite of the absence of external tube-tube contacts, a significant increase in loss modulus for the MWNT-PC system compared to the baseline PC is observed. In fact the response closely resembles the SWNT-PC system (figure 6b). Below ~ 0.2% strain amplitude (tube-matrix sliding is not activated), and the loss modulus of the nano-composite sample is close to the baseline PC. Above ~ 1% strain level, the loss modulus response levels off indicating that tube-matrix slip has been activated for a majority of the MWNT in the composite. This similarity in the response

of the two systems provides further evidence of a common mechanism (namely tube-matrix frictional sliding) that governs energy dissipation in our nanocomposite structures.

For the SWNT-PC composite, figures 8-9 indicates that nanotube dispersion is an important design parameter in terms of maximizing the frictional energy dissipation. This is because with improved dispersion of the nanotubes, the full impact of the SWNT's surface area of interaction comes into play and the effectiveness of the tube-polymer sliding dissipation mechanism is expected to improve significantly as a result of this. However it is very challenging to prevent the agglomeration of SWNT in a polymer matrix. The interfacial adhesion between SWNT and polycarbonate, which is caused by weak Van der Waals interaction, is generally not strong enough to achieve good quality dispersion of SWNT. To help alleviate this effect, as-received SWNT were oxidized by sonication in nitric acid. The resulting carboxylic groups on the SWNT help to exfoliate the nanotube bundles and also the intermolecular forces caused by dipole-dipole interaction between polar groups (i.e. carboxylic acid groups on the sidewall of nanotubes and the polar carbonate groups along polycarbonate chains), lead to better quality of dispersion. Indeed, SEM images of the samples (figure 10a and 10b) confirm that the oxidized SWNT-PC composite displays significantly improved dispersion compared to the as-received SWNT-PC composite. Test data for the loss modulus of the oxidized and as-received SWNT-PC composites is shown in figure 11 along with the baseline data for the pristine polycarbonate (without any fillers). For 1 wt% of SWNT, the oxidized SWNT-PC sample shows a maximum loss modulus of ~ 70 MPa compared to ~ 45 MPa for the as-received SWNT-PC sample: an increase of nearly 60%. Similar tests with

oxidized MWNT-PC composites showed only about 5% increase in loss modulus compared to as-received MWNT-PC samples. This indicates that since as-received MWNT are well dispersed in the polymer matrix, oxidation has a small influence on performance. In contrast, as-received SWNT are not very well dispersed (figure 10a) and therefore nanotube oxidation plays a strong role in improving dispersion quality (figure 10b) and hence the damping response.

Another approach to increasing the frictional energy dissipation is to boost the weight fraction of SWNTs in the composite. Figure 11 compares loss modulus data for oxidized SWNT-PC samples with 1% and 2% weight fraction of nanotube fillers. The loss modulus of the 2% weight fraction oxidized SWNT-PC sample at 1% strain amplitude is ~ 150 MPa compared to about 70 MPa for the 1% weight fraction sample. The 150 MPa loss modulus reported for the 2% weight fraction oxidized SWNT-PC system is more than an order of magnitude greater (> 1000%) than the baseline PC (~12 MPa). As far as being aware, this is the first time that order of magnitude changes in mechanical damping have been demonstrated in bulk polymer systems by the use of nanoscale fillers. Importantly the improvement in damping was engineered without compromising the elastic stiffness of the polymer; in fact the storage modulus of oxidized SWNT-PC was 10-20% greater than the pure PC sample (figure 12).

To confirm the nanotube-polymer sliding dissipation mechanism with other polymer systems we also performed viscoelastic uniaxial mode testing of SWNT-PEO (polyethylene oxide: Aldrich 182001-250G, Young's modulus: 0.8 GPa) composites, which are softer than SWNT-PC (Young's modulus: 2.35 GPa) composites. As shown in

figure 13, the same trends shown previously in figure 11 and figure 12 for SWNT-PC composites (i.e. a decrease in elastic modulus coupled with an increase in the loss modulus as the strain amplitude is increased) were also observed for SWNT-PEO composites, indicating that the nanotube-polymer sliding energy dissipation mechanism may be broadly applicable to a variety of polymer structures.

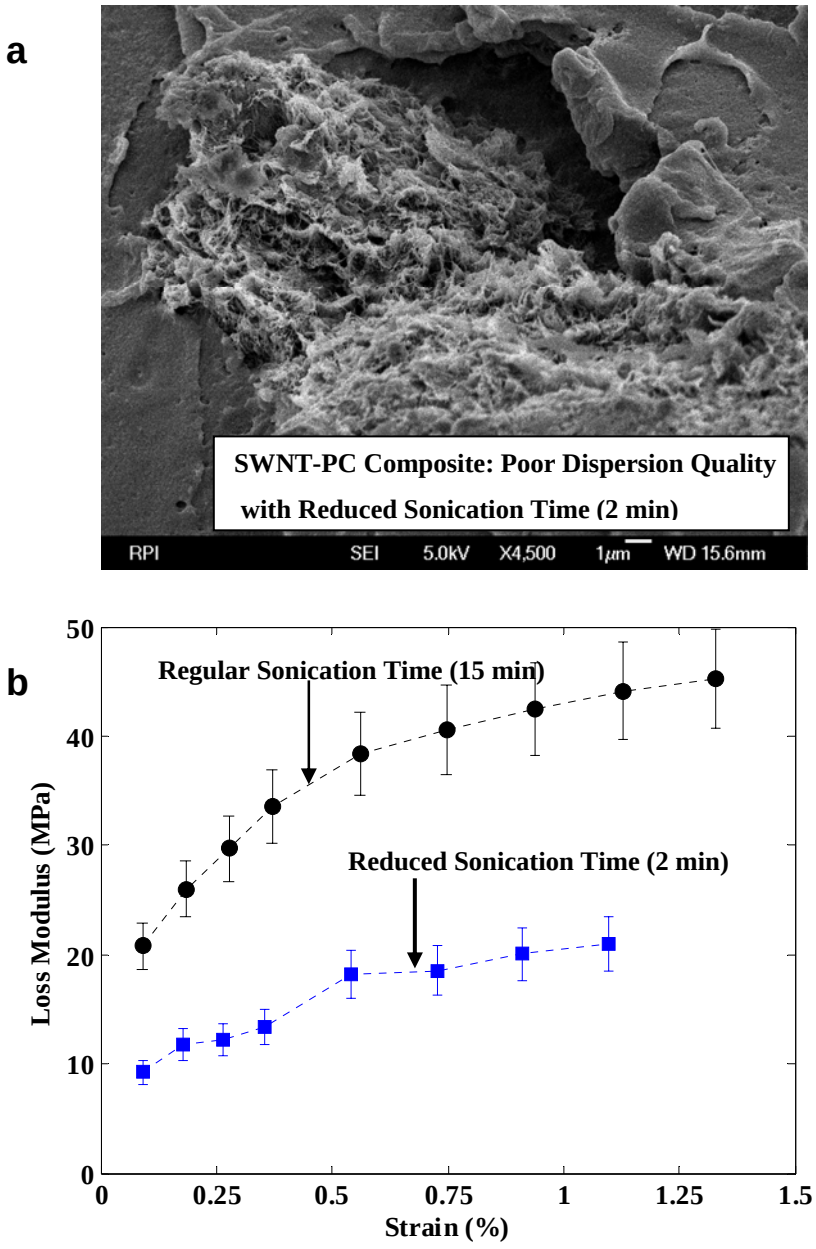

Figure 8: Effect of nanotube poor quality dispersion. (a) SEM image of the fracture surface of nanocomposite sample with reduced sonication time (2 min); the weight fraction of as-received SWNT in the sample is 1.5%. (b) Loss moduli of the control and reduced sonication time samples are plotted as a function of strain amplitude. (Test frequency: 10 Hz)

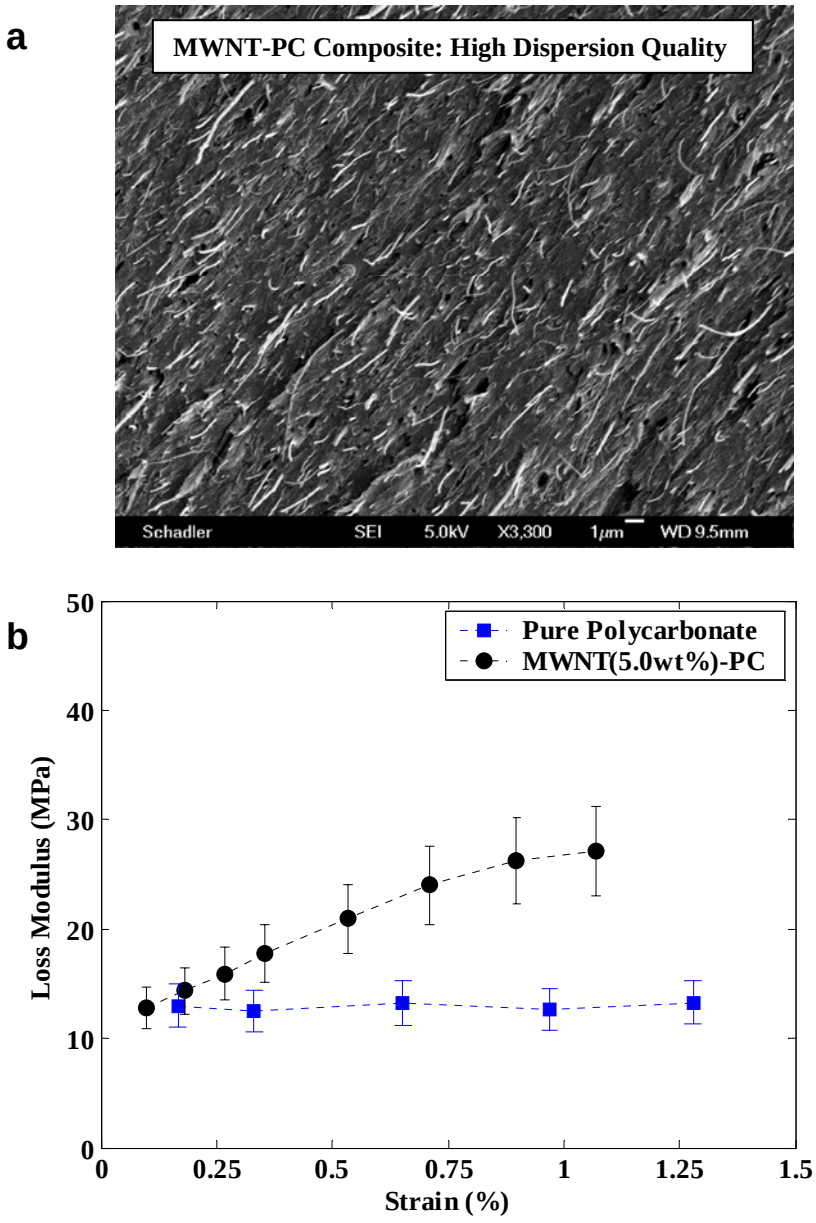

Figure 9: Effect of the nanotube high quality dispersion. (a) SEM image of MWNT-PC composite with 5% weight fraction of nanotube fillers. (Provided by Prof. Schadler) (b) Loss moduli of the MWNT-PC composite (5% weight fraction of nanotubes) and baseline PC are plotted as a function of strain amplitude. (Test frequency: 10 Hz).

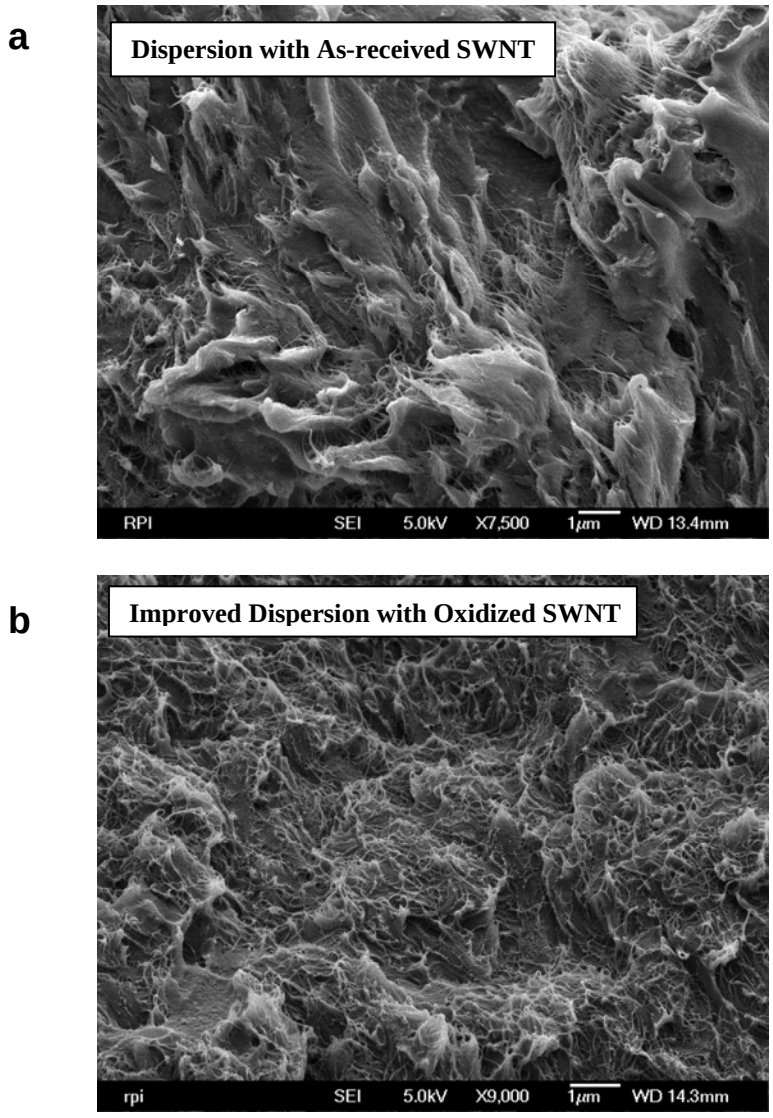

Figure 10: SEM images of the fracture surfaces (a) as-received SWNT-PC sample and (b) oxidized SWNT-PC sample.

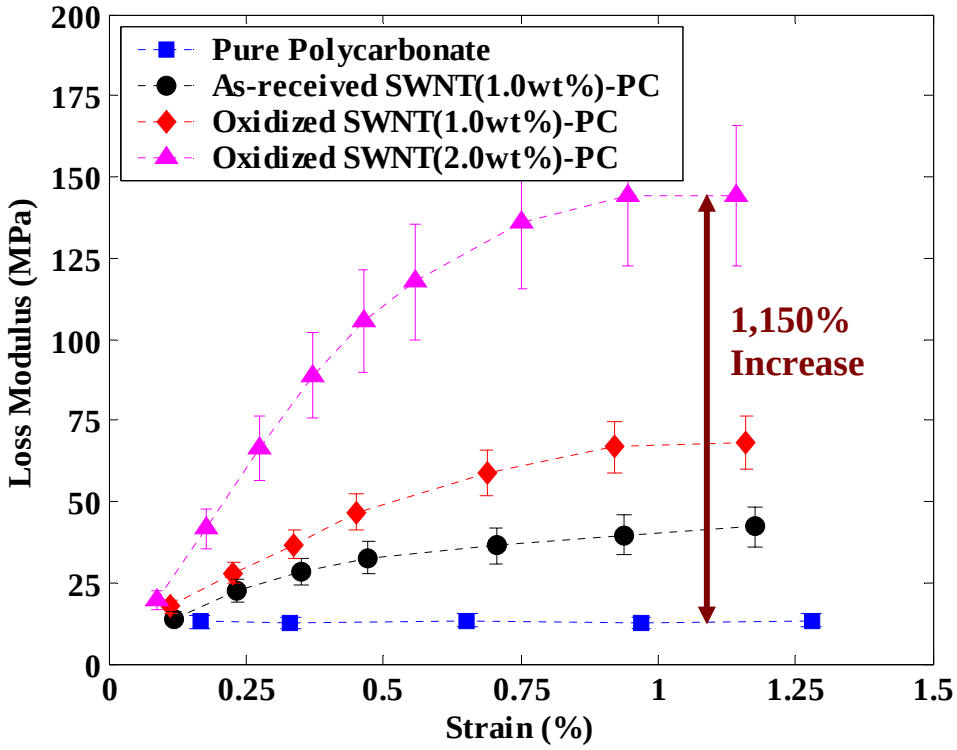

Figure 11: Loss moduli as a function of strain amplitude for pure polycarbonate, 1wt% as-received SWNT-PC, 1wt% oxidized SWNT-PC, and 2wt% oxidized SWNT-PC samples. (Test frequency: 10 Hz)

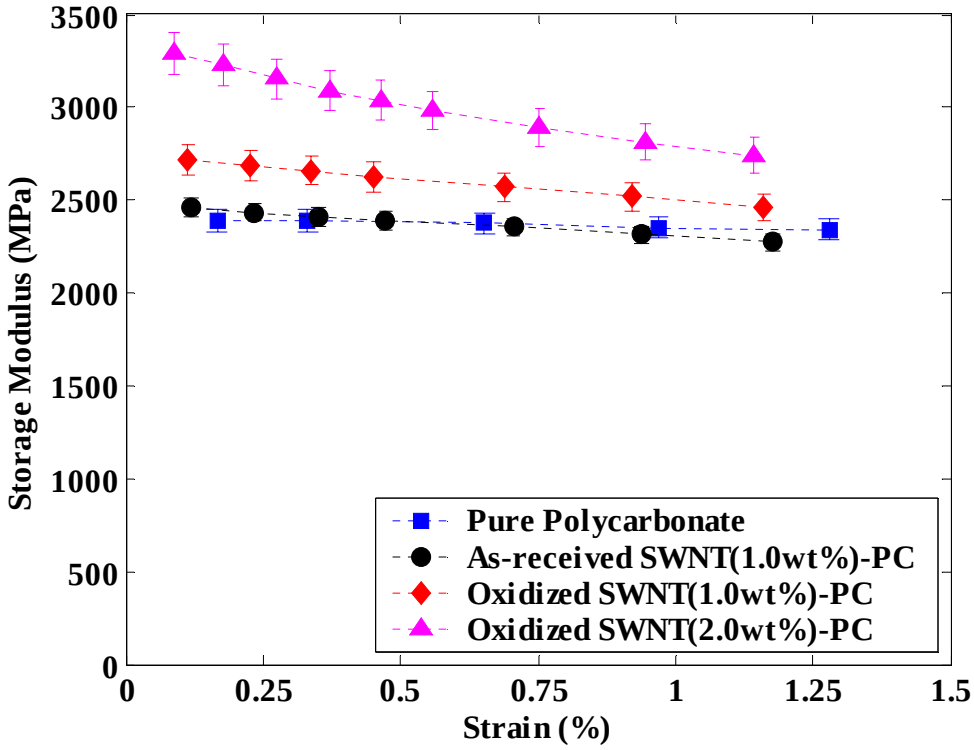

Figure 12: Storage moduli as a function of strain amplitude for pure polycarbonate, 1wt% as-received SWNT-PC, 1wt% oxidized SWNT-PC, and 2wt% oxidized SWNT-PC samples. (Test frequency: 10 Hz)

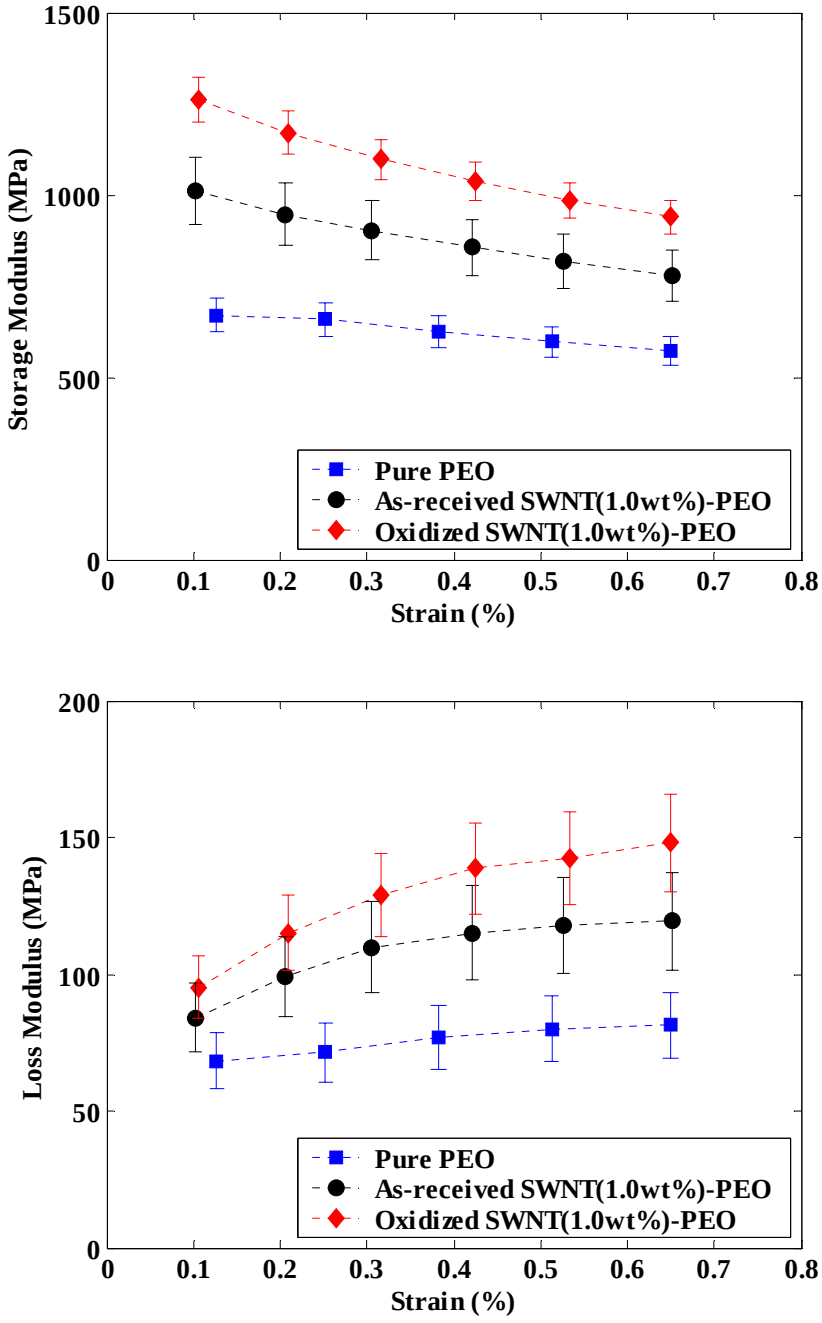

Figure 13: Storage (a) and loss moduli (b) as a function of strain amplitude for pure polyethylene oxide, 1wt% as-received SWNT-PEO, and 1wt% oxidized SWNT-PEO samples. (Test frequency: 10 Hz)

We have also studied the effect of establishing covalent linkages between the nanotubes and the polymer matrix. This was achieved using an epoxidation procedure. The carboxylic acid groups on oxidized nanotubes are used to enable covalent interactions between the nanotube fillers and the surrounding polymer chains. In this study, as-received SWNTs were first oxidized by the nitric acid treatment, as introduced previously, followed by a reaction with an epoxide- terminated molecule. These functionalized SWNTs were then able to react covalently with polycarbonate chains in the matrix.

The general schematic for the epoxidation of SWNTs in this study is illustrated in figure 14. The oxidized SWNTs and 200ml of butyl glycidyl ether (BGE) were mixed into a round flask. The mixture was sonicated for 20 minutes at room temperature. Then 5ml of trihexylamine (the catalyst) were added to the flask. While the mixture was stirred with a magnetic stirrer, and heated with an oil bath to 90ºC for 24 hours, the reaction proceeded between the oxidized SWNTs and BGE. Repeatedly, the product was then washed with acetone, and filtered through a 0.2μm PTFE membrane. Then the collected nanotubes were dried under vacuum oven at 50°C for 12 hrs. These epoxidized nanotubes can then react with the polycarbonate chains in the matrix, forming a covalent bond according to the scheme given in figure 14.

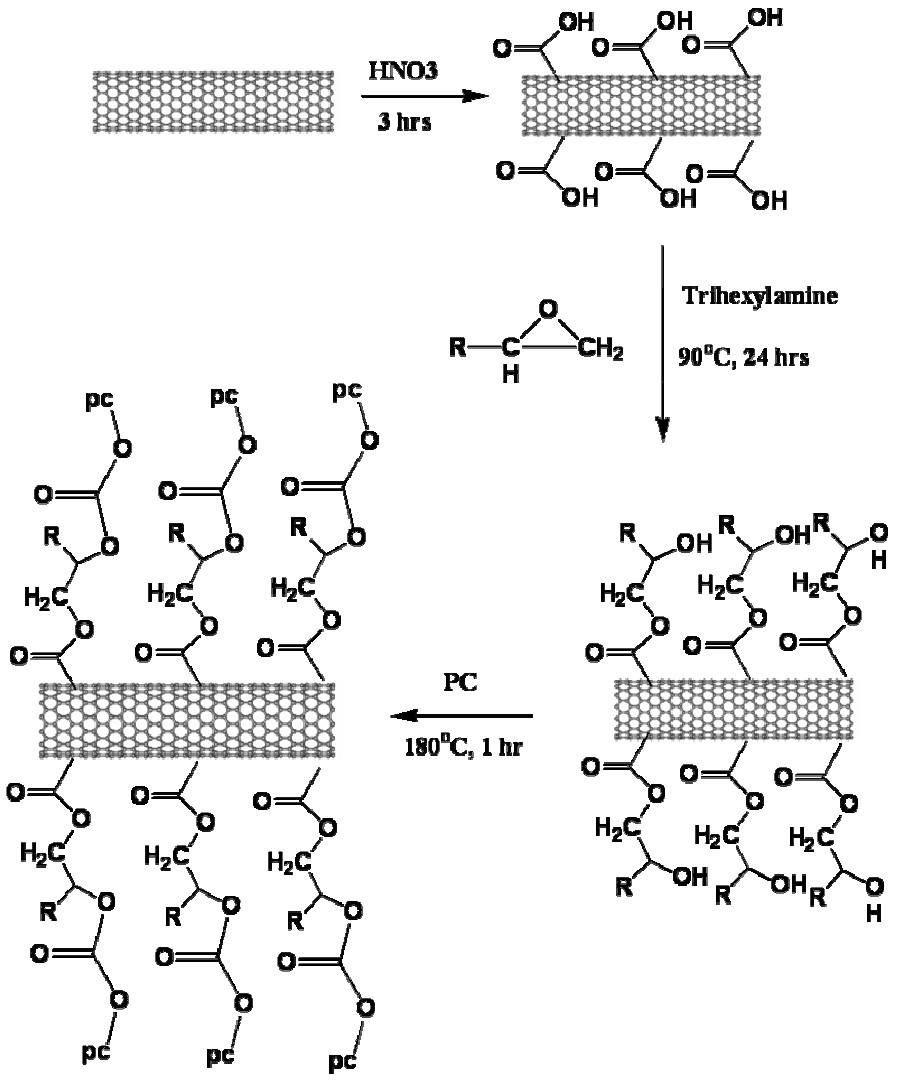

Figure 14: Schematic of the epoxidation of SWNTs.

Figure 15 compares the data for the storage and loss moduli of pure polycarbonate, 1wt% of as-received SWNT-PC, and 1wt% of epoxidized SWNT-PC composite samples at the test frequency of 1Hz. Figure 15a indicates that the epoxidized SWNT-PC composite shows significant reinforcement in the elastic moduli, compared to as-received SWNT-PC composite, which only have van der waals (non-bonding) type interactions or entanglements of the polymer chains, indicating that a covalent bond forms between the functionalized nanotube surfaces and surrounding polymer chain. Also, the loss in reinforcement with increasing strain amplitude is more gradual compared to as-received SWNT-PC composite sample, due to the stronger interfacial strength at the filler-matrix interfaces. As discussed earlier, as frictional sliding at the tube-polymer interfaces is activated, an increase in the loss modulus of nanocomposite sample is expected. This is clearly shown in figure 15b for as-received SWNT-PC composite sample. On the other hand, the epoxidized SWNT-PC samples shows relatively strain-independent loss moduli over the entire strain range, similar to the behavior of the pure polycarbonate sample. This indicates that stronger interfacial strength (as a result of covalent boning) can in fact inhibit filler-matrix sliding thereby lowering the damping response. In other words covalent bonding may in fact serve to prevent the activation of interfacial sliding leading to enhanced storage modulus but lower loss modulus (damping) response.

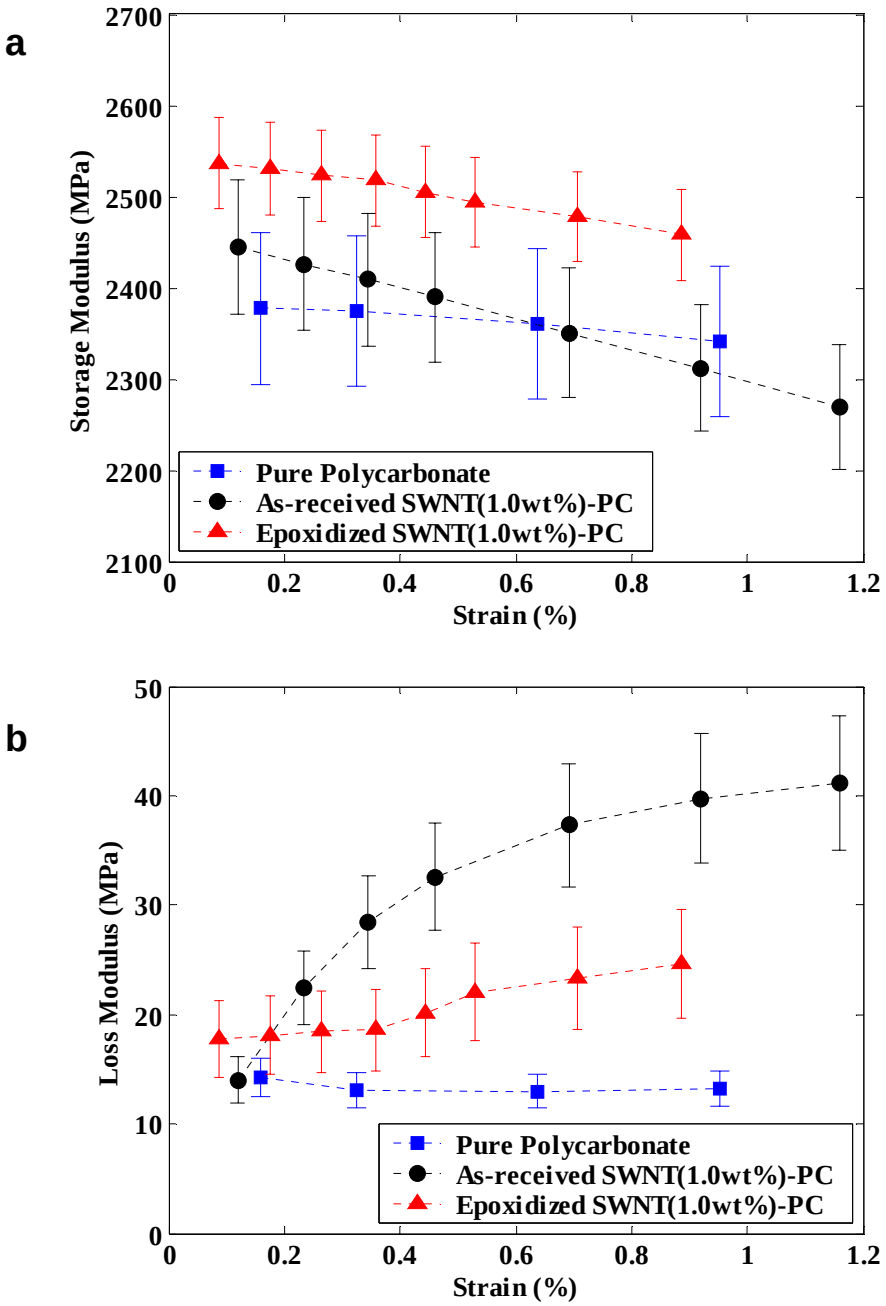

Figure 15: Storage (a) and loss moduli (b) as a function of strain amplitude for pure polycarbonate, 1wt% as-received SWNT-PC, and 1wt% epoxidized SWNT-PC samples. (Test frequency: 1 Hz)

We systematically investigated the effect of temperature on the nanotube-polymer sliding energy dissipation mechanism. It is well established that polymers undergo relaxation processes (associated with various modes of molecular motions) as the temperature is varied. Among the typical relaxation processes of amorphous polymers, α-relaxation has the characteristics of a glass transition (i.e. enhanced mobility of polymer backbones), while the β-relaxation process involves a local relaxation (i.e. motion of side groups attached to the polymer backbone). To study the effect of temperature, we raised the test temperature (using an MTS 651.05E environmental chamber) from room temperature to 90° C in steps of 15° C. Each temperature test was conducted at a fixed uniaxial strain amplitude of 0.35%. Figure 16a indicates that as the temperature is raised the storage modulus of the nano-composite shows a marked decrease from ~ 2,800 MPa at 30° C to ~ 2,500 MPa at 90° C. Similarly the nano-composite's loss modulus (figure 16b) increases with temperature from ~ 40 MPa at 30º C to ~75 MPa at 90º C. It is interesting to note that the nano-composite's storage modulus (for 0.35% strain amplitude) at 90º C is similar to its room temperature storage modulus at 1.2% strain amplitude. Similarly the nano-composite's loss modulus (for 0.35% strain amplitude) at 90º C is very close to its room temperature loss modulus at 1.2% strain. At room temperature, 1.2% strain corresponds to a level of strain where interfacial slip has been activated for a majority of the nanotubes within the composite. Therefore the fact that the storage and loss modulus of the nano-composite at 90º C and 0.35% strain is similar to that at room temperature and 1.2% strain, suggests that increasing temperature also

serves to activate interfacial slip, just as increasing the strain amplitude was shown to promote interfacial slippage. At elevated temperatures, as the glass transition temperature of the polymer (T_g ~ 145º C for polycarbonate) is approached, the mobility of the polymer chain backbones is enhanced. This can weaken the mechanical inter-locking between the nanotubes and the host structure matrix making it relatively easier to activate interfacial slip at a lower strain level. Another contributing factor could be the mismatch in the thermal expansion coefficient of the SWNTs and the host matrix material, which gives rise to a radial compressive stress at the tube-polymer interface. As the temperature is increased this radial compressive stress is relieved thereby weakening tube-matrix adhesion and facilitating the activation of interfacial slip.

We also measured the damping responses of the nano-composites and pure polycarbonate samples below room temperature. Figure 17a compares the data for loss moduli of the nano-composite and pure polycarbonate as a function of temperature in the 20 to -60^o C range. As the β-transition temperature of polycarbonate (~ -60° C) is approached, a significant enhancement in the damping behavior is observed for both the pure polycarbonate and the nano-composite samples due to increased mobility of the side chains in the polycarbonate. However the relative difference in loss modulus of the nano-composite and the baseline polycarbonate sample is not significantly affected by the β-relaxation of the polymer. This indicates that the increase in the energy dissipation associated with the β-relaxation effect of the polymer side chains is identical for both the nano-composite and the pure polycarbonate system. Figure 17b compares the effect of strain amplitude on the pure polycarbonate and nano-composite samples at room tem-

perature and at -60° C. At both temperatures, the nano-composite sample shows very similar sensitivity to the strain amplitude. This confirms the observation of figure 17a that side chain mobility of the host polymer matrix has a relatively small impact on promoting interfacial slip at the nanotube-matrix junctions.

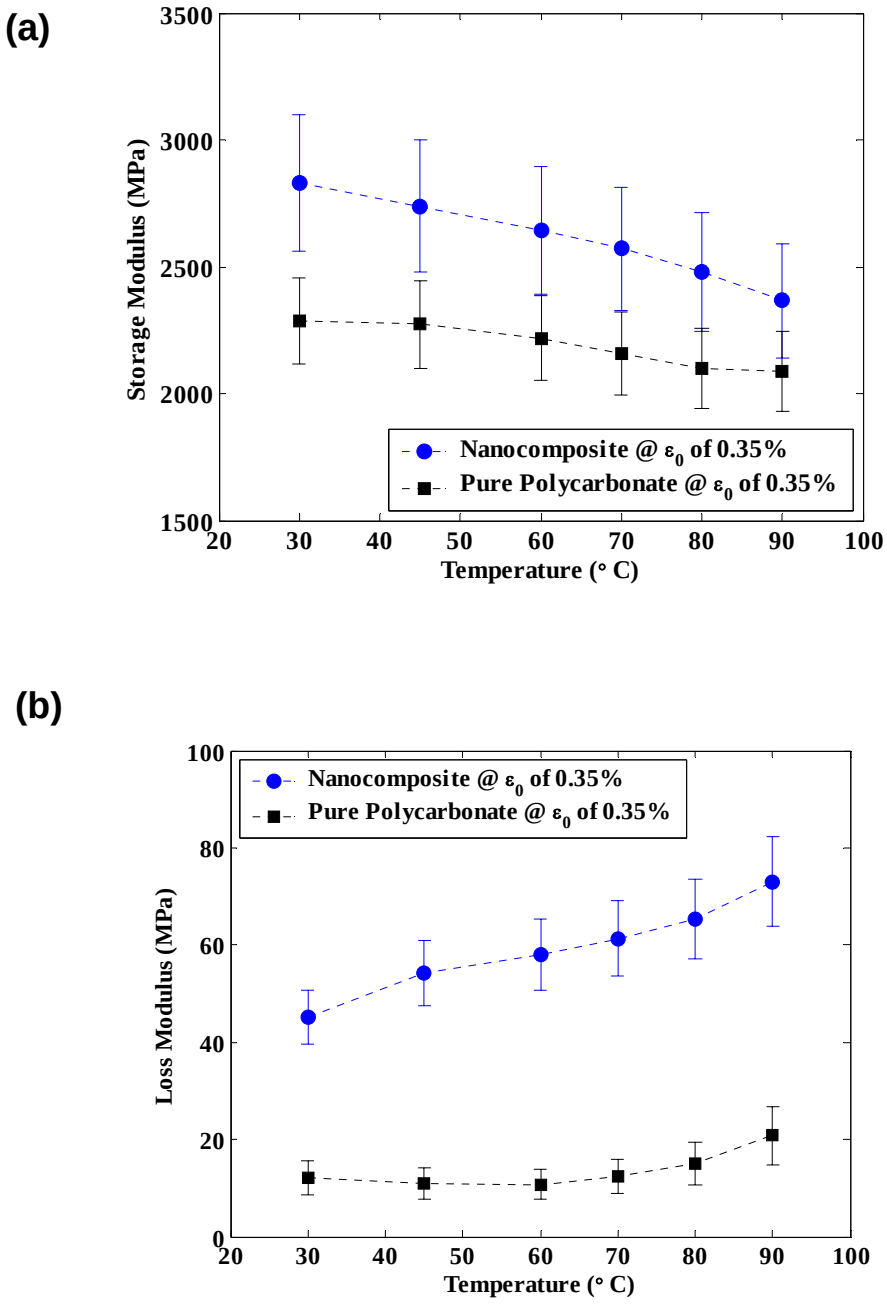

Figure 16: Storage (a) and loss moduli (b) as a function of temperature (above room temperature) for pure polycarbonate and 1.5wt% oxidized SWNT-PC samples. (Test frequency: 1 Hz)

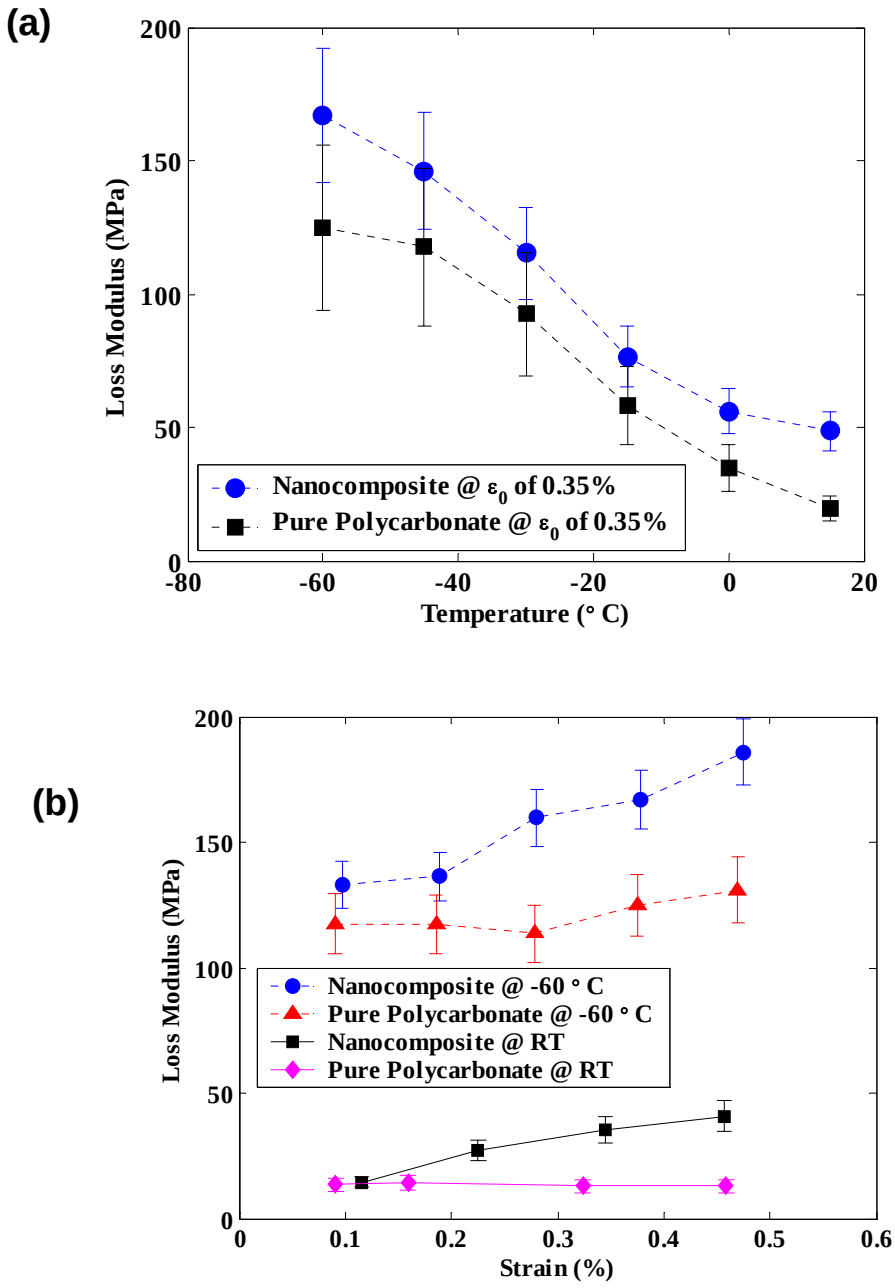

Figure 17: Storage (a) and loss moduli (b) as a function of temperature (below room temperature) for pure polycarbonate and 1.5wt% oxidized SWNT-PC samples. (Test frequency: 1 Hz)

Next, we proceeded to characterize the effect of pre-strain on the system response. This was carried out by superimposing a static pre-strain (ε_0: in 0.35 to 0.85 % range) on the dynamic strain (ε). The dynamic strain amplitude (ε) was held constant at 0.35% in all our tests. Figure 18a indicates that as the pre-strain is raised the storage modulus of the nano-composite shows a marked decrease from ~ 2,700 MPa at 0% pre-strain to ~ 2,450 MPa at 0.85% pre-strain. Similarly the nano-composite's loss modulus (figure 18b) increases with pre-strain from ~ 36 MPa at 0% pre-strain to ~ 50 MPa at 0.85% pre-strain. By contrast the storage and loss modulus of the pure polycarbonate sample (with no nanotube fillers) shows weak dependence on the pre-strain level.

The decrease in the storage (elastic) modulus and increase in loss modulus of the nano-composite with increasing pre-strain indicates that load transfer at the tube-polymer interfaces is degrading as the pre-strain is increased. This follows because as pre-strain (ε_0) is increased it augments the dynamic strain (ε) causing the cumulative (or peak) interfacial shear stress at the tube-polymer interfaces to increase.

In this project, we have characterized for the first time the effect of mechanical pre-strain on the interfacial friction damping properties of carbon nanotube polymer composites. We show that the damping properties of nanotube composites are significantly enhanced as the pre-strain levels are increased. At elevated pre-strains, interfacial nanotube-matrix slip can be activated at lower dynamic strain levels, thereby maximizing the energy dissipation capability of the system.

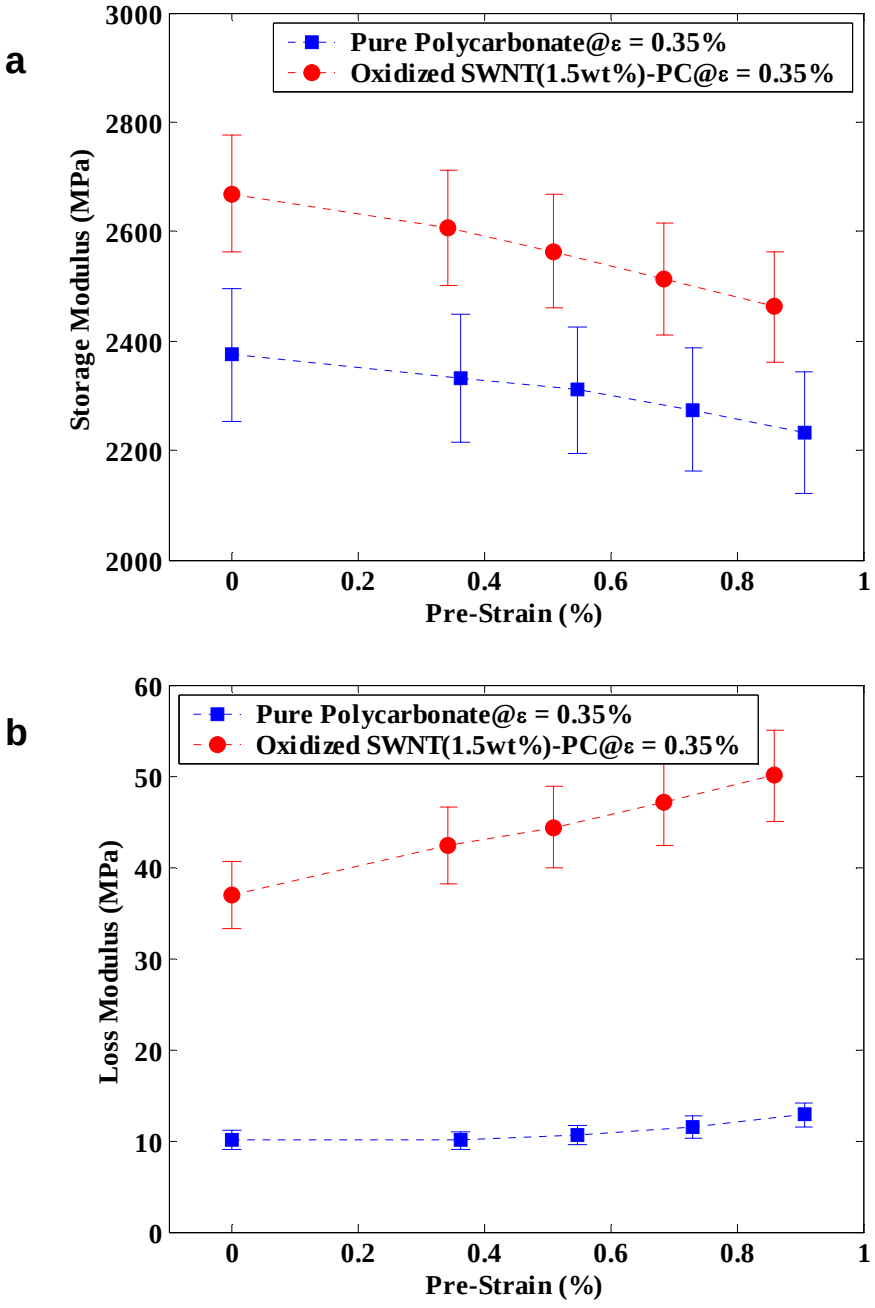

Figure 18: Storage (a) and loss moduli (b) as a function of pre-strain for pure polycarbonate and 1.5wt% oxidized SWNT-PC samples. (Test frequency: 1 Hz)

We also compared the damping response of carbon nanotube to that of nanoparticle fillers. An advantage of using nanoparticle fillers compared to carbon nanotubes in composites is that nanoparticles are significantly cheaper to produce in bulk quantities. Therefore if nanoparticles prove to be equally effective as nanotubes in dissipating energy, then nanoparticles will be more cost effective in introducing damping into bulk (macroscopic) structures. To investigate this, we studied the damping properties of C_{60} polycarbonate (PC) composites and compared them to single-walled nanotube (SWNT) polycarbonate composites. There are many similarities between SWNT and C_{60}. For instance fullerenes such as C_{60} display a very high surface area per unit volume similar to SWNT. In addition C_{60} and SWNT share a very similar surface chemistry. We therefore decided to investigate whether C_{60}-PC composites are equally effective at enhancing damping as nanotube-based composites. The difference between the two is aspect ratio (or length to diameter ratio). While spherical fullerenes such as C_{60} have an aspect ratio of 1.0, the 1-dimensional SWNT if dispersed down to the single tube level can display aspect ratios in excess of 1000. In this project we compare the damping response of C_{60}-PC and SWNT-PC systems with the same filler weight fraction (1%) and show that nanoparticles such as C_{60} are ineffective at damping enhancement due to their reduced aspect ratio.

Figure 19a and 19b show typical SEM images of the fracture surface of C_{60}-PC and SWNT-PC nano-composites with identical weight fraction (1%) of filler materials. As seen in the SEM images (Fig. 19a), C_{60} fullerenes are reasonably well dispersed in the polymer matrix, and the aggregates of C_{60} nanoparticles have an average diameter of ~10-15 nm. These nanoparticle clusters are well separated from each other as indicated

by the SEM pictures. Characterization of the SWNT-PC composite (Fig. 19b) shows that the average diameter (~30 nm) of the SWNT aggregates is also of the same order of magnitude as the C-60 aggregates. The manufacturer supplied length of the individual SWNT is ~1μm, therefore we expect that the length of the SWNT fibers to be at least 1 μm, resulting in a minimum aspect ratio (L/d: where L is the length and d is the diameter) of the nanotube fiber to be ~ 30. In contrast, the aspect ratio of spherical clusters of C_{60} nanoparticles is observed to be nearly 1.0, which is expected. The surface area to volume ratio of the C_{60} aggregates (~ 3×10^{8} m^{-1}) is about five times greater than that of the nanotube fibers (~ 5.7×10^{7} m^{-1}).

Figure 20 compares the material loss modulus (energy dissipation) response for the nanocomposite (C_{60}-PC and SWNT-PC) samples and the pure (baseline) polycarbonate. The weight fraction of C_{60} and SWNT in the composites is 1%. The pure polycarbonate sample shows strain-independent loss modulus behavior; this is to be expected since interfacial slippage is difficult to activate for the highly cross-linked polycarbonate chains. In contrast, the SWNT-PC composite shows strong amplitude-dependent damping behavior; as the strain amplitude is increased the energy dissipation, or loss modulus, is observed to increase sharply. As opposed to the SWNT-PC sample, the C_{60}-PC composite shows strain-independent loss modulus (~12 MPa) with no significant enhancement in loss modulus compared to the pure PC over the entire range of strain amplitudes.

To explain these results let us consider the energy loss (ΔW) that arises from interfacial slippage of one single filler in the matrix: $\Delta W=\int\tau_{o.}(\delta u).dS$, where τ_o is the critical interfacial shear stress, δu is the slipping distance and dS is the active area of the

filler that participates in the sliding. The critical stress (τ_o) depends only on van der Waals forces and is expected to be identical for the nanotube and the C_{60} additives. The slipping distance (δu) depends on the applied strain input and is the same for both additives. The difference between the two is in the active area (dS). The typical deformation profile around a particle inclusion under the action of a uniaxial load is shown in Fig. 21a. Both normal and shear stresses act on the particle; the normal stresses will cause extensive de-bonding to take place as shown in the schematic. The particle matrix contact is, therefore, a line contact and the active interfacial contact area (dS) is expected to be negligible. Similar to the particle case the end caps of the tubes will also debond under the action of normal stresses, but the majority of the tube length retains intimate contact with the matrix. As the applied load (or applied strain input) is increased the shear stress at the tube ends will increase; when the stress exceeds the critical stress (τ_o), the tube-matrix interface fails in shear causing the resin to slip over the tube (Fig. 21b). As interfacial slip proceeds along the length of the tube, the active area dS also increases; when the entire tube fails in shear the active area is equal to the surface area of the cylindrical portion of the tube. This area is significantly greater than that of the nanoparticle with its line contact and this explains why the nanotube is far more effective at dissipating energy than the nanoparticles.

(a)

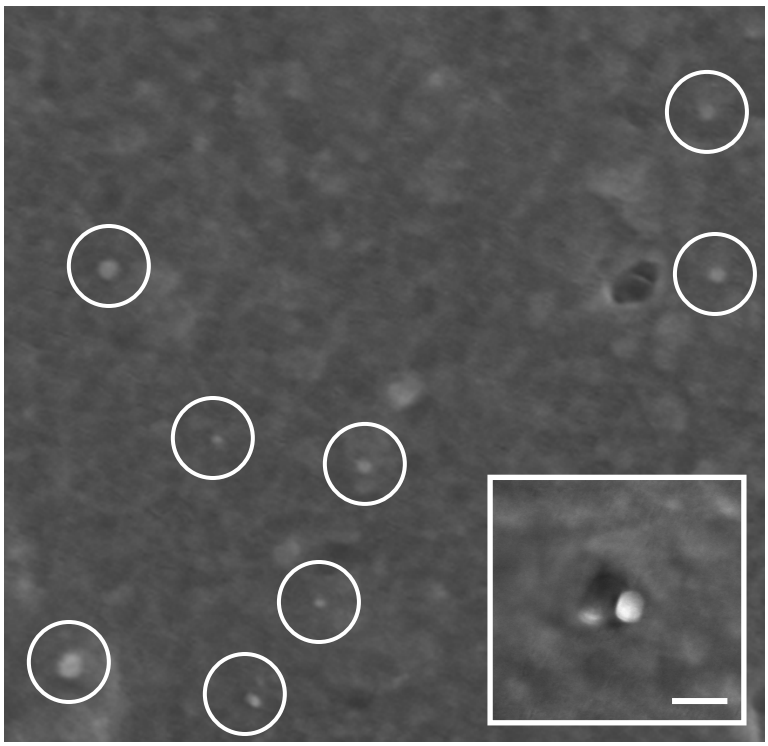

(b)

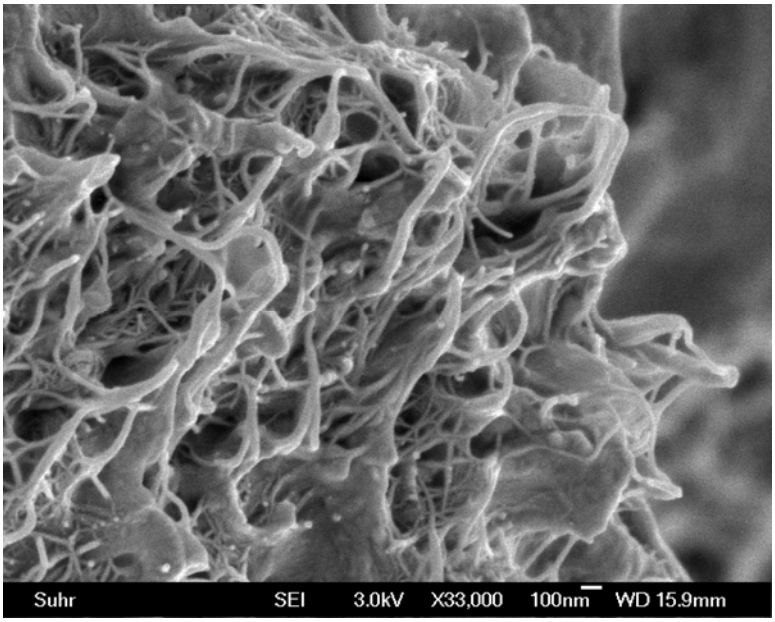

Figure 19: Microsctructure of C-60 composite (a) and nanotube composite (b).

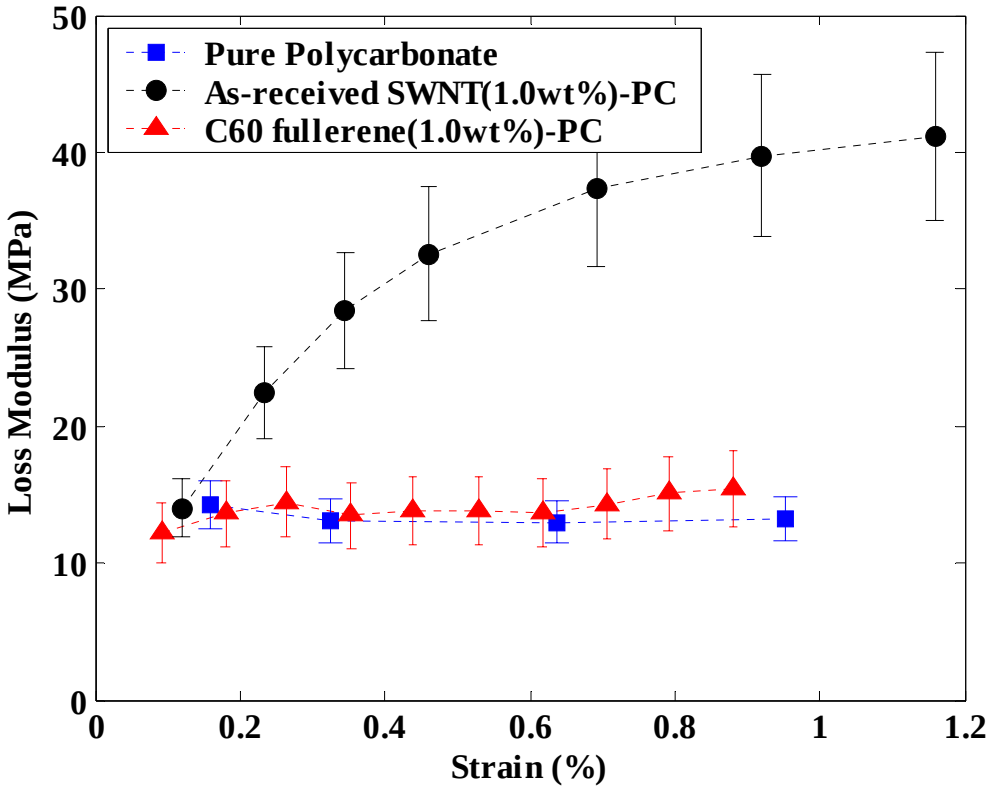

Figure 20: Results for loss modulus of C-60 nanocompoiste, nanotube-composite and pure polymer samples.

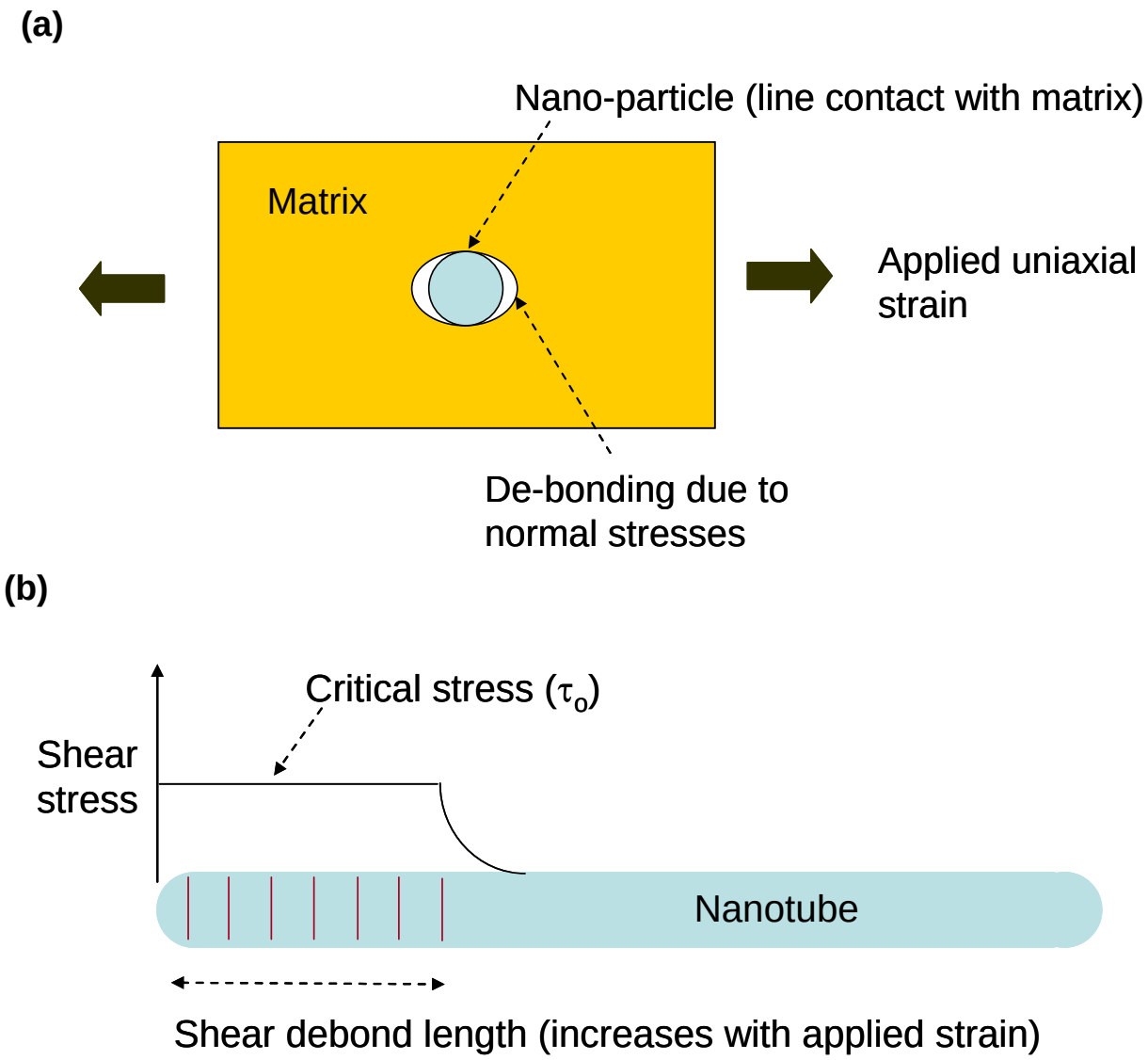

Figure 21: Concept schematic of deformation profile around a nano-particle inclusion (a) and nanotube inclusion (b).

Summary

In this project, singlewalled carbon nanotubes and bisphenol-A-polycarbonate composite beams are fabricated by a solution mixing process. We show that frictional sliding at the nanotube-polymer interfaces can deliver an order of magnitude (> 1000%) increase in loss modulus of the bulk polycarbonate system with only 2% weight fraction of oxidized SWNT fillers. The most dramatic increases in damping are reported at large strain amplitudes, when the tube-polymer adhesion is not strong enough to prevent interfacial slip. The damping behavior is also strongly influenced by the quality of dispersion and separation of the nanotubes in the polymer matrix, which supports the hypothesis of tube-polymer sliding as the dominant mechanism for energy dissipation in the bulk polymer composite system. We investigated the effect of temperature and observed that high temperature assists with the activation of tube-polymer sliding due to enhanced mobility of the polymer chains closer to the glass transition temperature. In contrast we observed that the establishment of covalent bonds at the nanotube-polymer interface inhibits the activation of tube-polymer sliding and serves to reduce the damping response. We also reported significant improvement in damping performance with the application of pre-strain as pre-strain similar to temperature also facilitates the activation of tube-polymer slip. Finally we compared the damping performance of nanoparticle additives to that of nanotube additives and showed that low aspect ratio nanoparticle additives are ineffective at damping enhancement.

Journal Publications from the ARO Award

1. J. Suhr, W. Zhang, P. Ajayan and N. Koratkar, "Temperature activated interfacial friction damping in carbon nanotube polymer composites", **Nano Letters** 6, 219 (2006).
2. J. Suhr, A. Joshi, L. Schadler, R. Kane and N. Koratkar, "Effect of Filler Geometry on Interfacial Friction Damping in Polymer Nano-Composites", **Journal of Nanoscience and Nanotechnology**; accepted for publication, in-press (2006).
3. W. Zhang, J. Suhr and N. Koratkar, "Carbon nanotube/polycarbonate composites as multifunctional strain sensors", **Journal of Nanoscience and Nanotechnology** 6, 960 (2006).
4. W. Zhang, J. Suhr and N. Koratkar, "Observation of high buckling stability in carbon nanotube polymer composites", **Advanced Materials** 18, 452 (2006).
5. J. Suhr and N. Koratkar, "Effect of pre-strain on interfacial friction damping in carbon nanotube polymer composites", **Journal of Nanoscience and Nanotechnology** 6, 483 (2006).
6. J. Suhr, N. Koratkar, D.-X. Ye and T.-M. Lu, "Damping properties of epoxy films with nanoscale fillers", **Intelligent Materials Systems and Structures** 6, 255 (2006).
7. J. Suhr, N. Koratkar, P. Keblinski and P. Ajayan, "Viscoelasticity in carbon nanotube composites," **Nature Materials** 4, 134-137, (2005).

8. N. Koratkar, J. Suhr, A. Joshi, R. Kane, L. Schadler, P. Ajayan, and S. Bartolucci, "Characterizing energy dissipation in single-walled carbon nanotube polycarbonate composites", **Applied Physics Letters** 87, 063102 (2005).
9. N. Koratkar, B. Wei and P. Ajayan, "Multifunctional structural reinforcement featuring carbon nanotube films", **Composites Science and Technology** 63, 1525-1531, (2003).
10. W. Zhang, J. Kim and N. Koratkar, "Energy-absorbent composites featuring embedded shape memory alloys" **Smart Materials and Structures** 12, 642-646, (2003).
11. N. Koratkar, B. Wei, and P. Ajayan, "Carbon nanotube films for damping applications", **Advanced Materials** 14, 997-1000, (2002).

Conference Publications from the ARO Award

1. "Characterization of multiwalled carbon nanotube polymer composites", J. Suhr, N. Koratkar, L. Schadler, In proceedings of the *SPIE's 12th International Symposium on Smart Structures and Integrated Systems*, San Diego, CA, March 6-10, (2005).

2. "Comparing damping properties of singlewalled and multiwalled carbon nanotube polymer composites", J. Suhr, L. Schadler, P. Ajayan and N. Koratkar, In proceedings of *46th AIAA/ASME/ASCE/AHS Structures, Structural Dynamics and Materials Conference*, April 18-21, Austin, Texas, (2005).

3. "Viscoelastic characterization of carbon nanotube thin films", J. Suhr and N. Koratkar, In proceedings of the *SPIE's 11th International Symposium on Smart Structures and Integrated Systems*, San Diego, CA, March 14-18, (2004).

4. "Damping properties of carbon nanotube films" E. Lass and N. Koratkar, In proceedings of the *SPIE's 10th International Symposium on Smart Structures and Integrated Systems*, San Diego, CA, March 2-6, (2003).

5. "Engineered connectivity in nanotube systems for damping applications," E. Lass and N. Koratkar, In proceedings of *MRS Fall Meeting*, 740, December 2-6, (2002).

6. "Shape memory alloy reinforced multi-functional composites", W. Zhang, M. Davis and N. Koratkar, In proceedings of *SPIE's 9th International Symposium on Smart Structures and Integrated Systems*, March 18-21, San Diego, CA (2002).

7. "Novel carbon nanotube damping films", N. Koratkar, B. Wei and P. Ajayan, In proceedings of the *43rd AIAA/ASME/ASCE/AHS Structures, Structural Dynamics and Materials Conference*, April 22-25, Denver, Colorado (2002).

Students Graduated

Jonghwan Suhr- Ph.D.

Dr Suhr is presently a tenure track assistant professor in the Mechanical Engineering Department at the University of Nevada at Reno.

Interaction with Army Labs and Synergistic Activities

• Presented a seminar to Army Scientists (Dr Eric Kathe and Dr Andrew Littlefield of US Army, TACOM-ARDEC Benet Laboratories). The presentation described the ARO project in detail and was followed by a comprehensive discussion on various aspects of the proposed work.

• Published a paper on nano-composite damping materials in Applied Physics Letters Journal in collaboration with Dr. Steve Bartolucci of US Army, TACOM-ARDEC Benet Laboratories. Benet is now looking at this technology for ceramic composites used as high temperature materials in gun systems.

• Established contact with Dr Eric H. Anderson of CSA Engineering and discussed with him the details of the carbon nanotube damping project. We discussed potential collaboration between RPI and CSA Engineering with respect to comparing the damping performance of nanostructured materials with CSA's in-house damping treatments.

• Presented a seminar on Nanoscale Science and Technology at the DARPA sponsored Workshop entitled, "Nano Air Vehicles for Sensor Emplacement", Lansdowne, VA, March 2-3, (2004). The presentation was attended by leading scientists from academia, industry and army research laboratories.

• Invited lecture on carbon nanotube damping treatments at Materials Research Society Spring Symposium in San Francisco, CA, (2005).

• Organized special sessions on "Carbon Nanotubes and its Applications" at the SPIE's 11^{th}, 12^{th}, 13^{th} and 14^{th} International Symposia on Smart Structures and Integrated Systems. This was the first time that dedicated sessions on carbon nanotubes were introduced at the conference. These sessions were heavily attended by researchers from academia, government and industry.